FERMILAB-CONF-13-702-AD-APC

ENERGY DEPOSITION AND SHIELDING STUDY OF THE FRONT END FOR THE NEUTRINO FACTORY

Pavel Snopok*, Illinois Institute of Technology, Chicago, Illinois 60616, USA
David Neuffer, Fermilab, Batavia, Illinois 60510, USA,
Chris Rogers, Rutherford Appleton Laboratory, Chilton, Didcot, Oxon, UK

Abstract

In the Neutrino Factory and Muon Collider muons are produced by firing high energy protons onto a target to produce pions. The pions decay to muons which are then accelerated. This method of pion production results in significant background from protons and electrons, which may result in heat deposition on superconducting materials and activation of the machine preventing manual handling. In this paper we discuss the design of a secondary particle handling system. The system comprises a solenoidal chicane that filters high momentum particles, followed by a proton absorber that reduces the energy of all particles, resulting in the rejection of low energy protons that pass through the solenoid chicane. We detail the design and optimization of the system and energy deposition and shielding analysis in MARS15.

HIGH POWER MUON ACCELERATORS

In the proposed Neutrino Factory [1] facility, a multi-megawatt proton beam is fired onto a target to produce pions. The pions are captured in a high field solenoid that tapers to a 1.5 T constant field solenoid. Pions and their decay products, the muons, are allowed to drift longitudinally in this constant field solenoid and subsequently a variable frequency RF system is used to bunch and then phase rotate the muons. Muons are then passed into an alternating focusing ionization cooling system before acceleration to high energy. The Muon Collider facility has a similar capture system, although the proposed ionization cooling system is considerably more extensive in order to reach the very low emittances required for a high luminosity collider.

In this paper, we continue the study of the effect of undesirable secondary particles exiting the target region and passing through the subsequent muon capture systems. Losses are concentrated around the start of the ionization cooling channel where the magnetic lattice produces large transverse losses and the presence of Lithium Hydride absorbers for ionization cooling takes energy from electrons and protons. Losses are 100 W/m throughout the length of the front end and peak at several kW/m at the start of the cooling channel. Such high losses would certainly prevent hands on maintenance throughout the entire cooling channel, may cause radiation damage to equipment and quenching of superconducting magnets.

Two components are foreseen for a particle selection scheme: a chicane to remove high momentum particles from the beam; and a Beryllium plug that reduces momentum of all particles in the beam, resulting in the loss of low momentum protons. We concentrate here on energy deposition and shielding of the chicane.

CHICANE DESIGN

Given that it is challenging to get good transmission over the desired range of momenta, and that both positive and negative muon species need to be captured, a stellarator-type solenoidal chicane is proposed. Solenoidal chicanes induce a vertical dispersion in the beam, resulting in symmetric transmission of both particle charges. Matching from the constant solenoid field of the front end to the bent solenoid field is relatively easy. The main problem with this sort of lattice is that it is not possible to make an open midplane solenoid. Either very high radius superconducting coils with significant shielding or normal conducting coils exposed to beam power in the hundred kW range are required. Clearly these components would become active and it is expected that they would be treated as part of the remote handling facility in the target area.

The addition of a Beryllium proton absorber after the chicane serves to lower the overall energy of particles in the system. This has a more significant effect on the protons that pass the chicane, stopping almost all of them, while leaving most muons in the beam. Increasing the absorber thickness and increasing the chicane angle reduce the good muon yield slightly, while producing a dramatic reduction in the proton beam power escaping the system. Based on that, a 12.5° chicane angle and 100 mm proton absorber thickness were chosen.

CHICANE ENERGY DEPOSITION STUDIES

The chicane as simulated in MARS15 [2] and shown in Figure 1 starts at the end of the target/capture region, 30 meters downstream from the target, which corresponds to zero in Fig. 1. Field maps for MARS simulations were generated by G4beamline [3]. Coils have inner radius of 43 cm, outer radius of 53 cm, length of 18 cm, with on-axis field of 1.5 T throughout the channel. Either copper or a standard MARS material SCON consisting of 90% superconductor (60% Cu and 40% NbTi) and 10% Kapton ($C_{22}H_{10}N_2O_5$) are used for simulations. The proton absorber is a 10 cm Be disk of outer radius of 30 cm.

The current iteration of shielding assumes a stainless steel pipe at the radii of 30-32 cm and 36-38 cm to enclose

* psnopok@iit.edu

ISBN 978-3-95450-122-9

Operated by Fermi Research Alliance, LLC under Contract No. De-AC02-07CH11359 with the United States Department of Energy.

Copyright © 2013 by JACoW — cc Creative Commons Attribution 3.0 (CC-BY-3.0)

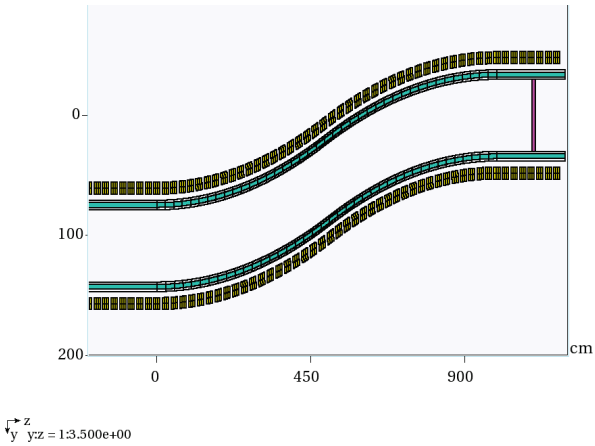

Figure 1: Chicane as simulated in MARS, top view. Yellow: solenoidal coils, cyan: W shielding, gray: SS beam pipe and shield pipe around W shield, magenta: 100 mm Be proton absorber.

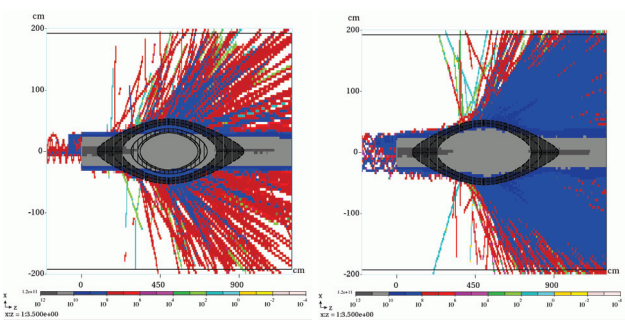

Figure 2: Comparison of the chicane with and without shielding inside the coils. Left: shielding vessel starts at the radius of 30 cm; right: no shielding, the spread is limited only by the coil inner radius of 43 cm.

the W shielding, yet stay 5 cm clear of the coils. This arrangement is not perfect, since it limits the shielding thickness. Also, the inner radius of the bore is not large enough to accommodate the full width of the muon beam at the point where the separation between positive and negative sign muons is at its largest. Figure 2 clearly shows that in the absence of shielding a much larger radius can propagate through the chicane. Hence, the shielding pipe needs to be elliptical rather than circular in order to accommodate more muons. Both of these questions will be addressed in the future.

The case of a chicane without shielding is used as a reference. In this case the peak total deposited power density in the coils is 15.8 mW/g, while a common limit for superconducting coils is 0.15 mW/g). In terms of peak linear power density for the geometry described above that corresponds to 42.6 kW/m for Cu coils, see Fig. 3, or 33.3 kW/m for SCON coils. That is significantly larger than the typical 1 W/m limit for hands-on operation. Since these numbers represent averages over the whole coil, a more thorough analysis is required by subdividing the coils into smaller

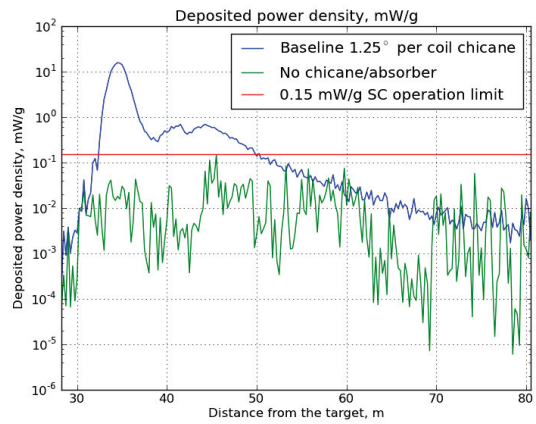

Figure 3: Energy deposition in the coils of the chicane with no shielding, mW/g, nominal 12.5° chicane, used as a reference.

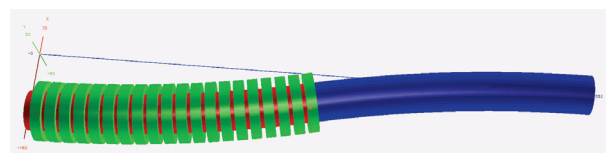

Figure 4: Chicane geometry as defined using ROOT. Red: shield, bend in; blue: shield, bend out; green: half of all the solenoidal coils.

segments in order to localize energy deposition peaks.

MARS Simulations, ROOT framework

Given the complicated geometry of the chicane, adding tungsten shielding was not straightforward using only MARS extended geometry. However, a recently developed ROOT-based geometry framework for MARS has made the task manageable with a wide variety of basic volumes provided by the ROOT TGeo module. The TGeoCtub elementary volume (cut tubes with arbitrary entrance and exit angles) proved to be the most important for seamless shielding. The fact that the volume of each shielding or coil segment can be calculated precisely in ROOT removes the uncertainty intrinsic to MARS Monte-Carlo based volume calculation. Parts of the chicane as defined using ROOT are shown in Fig. 4.

Shielding effect and coil segmentation

For a more in-depth analysis of energy deposition each coil was represented as a set of segments: 12 azimuthal segments (uniform, 30° each), 2 radial segments (at radii 43-48 and 48-53 cm), and finally 3 longitudinal segments (6 cm each), for a total of 72 segments per coil. As expected, even though the average energy deposition per coil is reduced dramatically with the introduction of shielding, there are peaks in the individual segments, since energy deposition is not uniform, especially where high energy protons left in the beam after the target exit the chicane, see

Copyright © 2013 by JACoW — cc Creative Commons Attribution 3.0 (CC-BY-3.0)

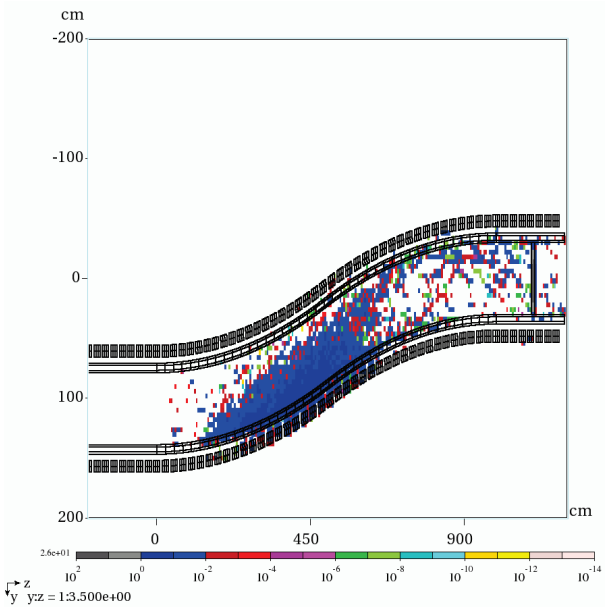

Figure 5: Non-uniform energy deposition in the coils, protons.

Fig. 5. Figure 6 illustrates the results of non-uniformity of energy deposition. Quantitatively, the average deposited power density in the coils is at maximum 1.7 mW/g as opposed to 15.8 mW/g with no shielding. At the same time, certain coil segments can get up to 9.1 mW/g.

CONCLUSIONS

A particle selection system has been designed for the Neutrino Factory and Muon Collider that reject secondary particle contaminants that would otherwise irradiate large parts of any subsequent acceleration system. The particle selection system has been shown to reject up to 99.9% of proton contaminants as well as creating a better conditioned muon beam at the expense of a slight reduction in muon yield. 4 cm of W shielding reduce energy deposition in the coils significantly, nonetheless, coils between 32 and 36 m downstream of the target will have to be replaced by normal-conducting ones in order to withstand power density up to 9.1 mW/g. The shape of the beampipe needs to be optimized in order to improve muon transmission.

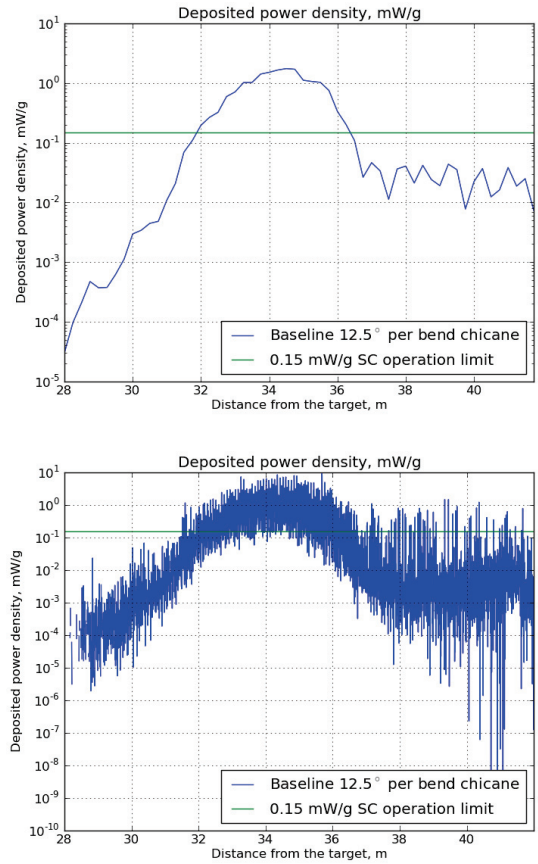

Figure 6: Chicane with 4 cm of W shielding. Top: average deposited power density per coil, max = 1.7 mW/g. Bottom: deposited power density for individual coil segments, max = 9.1 mW/g.

REFERENCES

[1] Choubey S. et al., International Design Study for the Neutrino Factory: Interim Design Report (2011), arXiv 1112.2853 [hep-ex]

[2] MARS Code System, http://www-ap.fnal.gov/MARS/

[3] T. J. Roberts et al, G4beamline Particle Tracking in Matter Dominated Beam Lines, p. 373–375, Proc. PAC 2011.

Copyright © 2013 by JACoW — cc Creative Commons Attribution 3.0 (CC-BY-3.0)

ISBN 978-3-95450-122-9